Exciton Dynamics within Quantum Dots

Anuj Krishnasundar Pennathur

A dissertation submitted for the partial fulfillment of the BS-MS dual degree in Science

Indian Institute of Science Education and Research Mohali

April 2017

Certificate of Examination

This is to certify that the dissertation titled "**Exciton Dynamics within Quantum Dots**" submitted by **Mr. Anuj Krishnasundar Pennathur** (Reg. No. MS12011) for the partial fulfillment of BS-MS dual degree programme of the Institute, has been examined by the thesis committee duly appointed by the Institute. The committee find the work done by the candidate satisfactory and recommends that the report be accepted.

Dr. Sabyasachi Rakshit Dr. Ujjal K. Gautam Dr.Arijit K. De

(Supervisor)

Declaration

The work presented in this dissertation has been carried out by me under the guidance of Dr. Arijit K. De at the Indian Institute of Science Education and Research Mohali.

This work has not been submitted in part or in full for a degree, a diploma, or a fellowship to any other university or institute. Whenever contributions of others are involved, every effort is made to indicate this clearly, with due acknowledgement of collaborative research and discussions. This thesis is a bonafide record of original work done by me and all sources listed within have been detailed in the bibliography.

Anuj Krishnasundar Pennathur

(Candidate)

Dated: April 21, 2017

In my capacity as the supervisor of the candidate's project work, I certify that the above statements by the candidate are true to the best of my knowledge.

Dr. Arijit K. De

(Supervisor)

Acknowledgements

First and foremost, I would like to express my deepest thanks to Dr. Arijit K. De for all of the insightful discussions (technical and general), constant motivation and a lot of intellectual freedom which I believe really helped me thrive.

Dr. Angshuman Ray Choudhary for graciously letting us use his lab for synthesis. Dr. Samrat Mukhopadyay for allowing us to use the TCSPC. Dr. Sharvan Sherawat for letting us use his centrifuge. Dr. Shantanu Pal for allowing us to use the DLS. Dr. Sabyasachi Rakshit and Dr. Ujjal Gautam for their helpful comments regarding this project.

I would like to thank my lab mates, for engaging discussions, instructive debates and inspiration; Dr. Somrita Mondal, Ms. Yogita Silori, Ms. Anita Devi, Ms. Shaina Dhamija, Ms.Monika Dahiya, Pragya Verma, Meghanad Kayanattil and Anusree P.V.

IISER Mohali for all of the instrumental facilities. The library for access to a plethora of journals.

I thank my friends and family for constant support.

List of Figures

List of Tables

Abbreviations

FRET: Förster’s resonance energy transfer

PPC: Pigment protein complex

FMO: Fenna-Mattews-Olson

TCSPC: Time-correlated single photon counting

λ_{ex} : Excitation maximum from UV-Visible spectroscopy

λ_{eo} : Emission maximum from fluorescence emission spectroscopy, with excitation at 485nm

λ_{e2} : Emission maximum from fluorescence emission spectroscopy, with excitation at 400nm

Contents

Abstract

We have tried to understand the role of excited state dynamics, particularly the transfer of excitation energy. The system which we worked with were cadmium selenide quantum dots, as they absorb in the visible region of the electromagnetic spectrum and have bandgap tunability based on their size. The primary techniques which were used to characterize the quantum dots were UV-Vis spectroscopy, fluorescence spectroscopy and time correlated single photon counting.

Excitation of quantum dots, can be described in terms of electron-hole pairs; excitons. As the time scales of excited state transfer of 2-4 nm CdSe quantum dots is on the order of a few pico seconds to a few tens of pico seconds, we had to use time resolved spectroscopy to understand these dynamics. We used visible pump-probe/transient-absorption spectroscopy to give us the rates, and consequently, time scales of the excited state charge transfer process.

Chapter 1: Introduction

With the global consumption of non-renewable energy being at an all-time high, we are on the verge of an energy shortage. This has caused attention to be drawn towards renewable sources of energy. Of the various choices of such sources, solar energy shows the most potential in terms of the amount of energy that can be harnessed as well as being more risk-free than the other renewable sources.

The model systems for light harvesting are plants. Plants drive all of our energy consumption, either directly or indirectly, through photosynthesis. The first step of photosynthesis is the collection of light from the sun. Light harvesting in plants happens in PPCs which are located in thylakoid membranes. PPCs consist of many different pigments, with their own characteristic absorption in the visible region, usually; chlorophyll, carotenoids and phycobilins. These pigments function in tandem, optimizing the spectrum of light harvested [1].

Light from the sun causes excitations of these pigments, this excitation is then funneled, initially through molecules of the same PPC and subsequently, from one PPC to another, until the excited energy reaches a special kind of PPC known as the reaction centre. At the reaction center, the excitation energy is changed into a charged separated state; the excited electron is abstracted to continue a chain of transfer reactions that drive photosynthesis. The efficiency with which sunlight is harvested is as high as 99% in certain organisms. This implies that almost every incident photon makes it to the reaction centre.

Initially excitation energy transfer was believed to be a purely incoherent process; hopping of excitation from one pigment molecule to another, localizing the excited energy to a single pigment molecule at a time. This scheme is similar to FRET. FRET is seen under three conditions [2]:

- The emission spectrum of the donor should overlap with the emission spectrum of the acceptor
- The distance between the donor and acceptor should be 10Å-100Å
- The orientations of the transition dipoles of the donor and acceptor should be favourable for overlap.

Recently, a new kind of energy transfer was observed when molecule-molecule distance was <10Å. In this case, the incident light would see an effective dipole moment for more than one molecule, so excitation would be delocalized by the molecules whose effective dipole was excited. These molecules which appear like an effective dipole, are termed molecular excitons. The number of molecules in an exciton depends on the concentration of molecules as well as the coupling between molecules. The dynamics of coherent energy transfer are best described in the exciton basis; where the basis functions are superpositions of molecular orbitals of the molecules involved in forming the exciton. This energy transfer came to be known as coherent energy transfer/redfield theory.

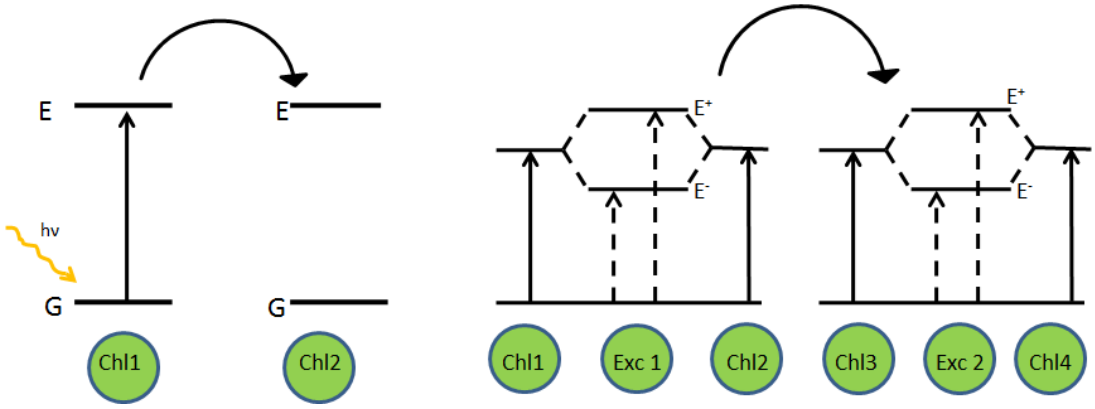

Fig1:(a) Incoherent excitation in the site basis, the basis vectors are molecular orbitals of each pigment. (b) Coherent excitation in the exciton basis.

In 2007, Graham Fleming and coworkers did a time resolved experiment on the FMO complex of green sulphur bacteria [3]. At 77K they saw persistent beats between pigments, indicative of a coherent energy transfer. With the help of 2D electronic spectroscopy, it was further shown that the pigment-pigment coupling involved in a molecular exciton persists for a long time (~650fs). This was not the first-time coherent energy transfer was reported, it was the first time that long-lived coherent energy transfer was reported.

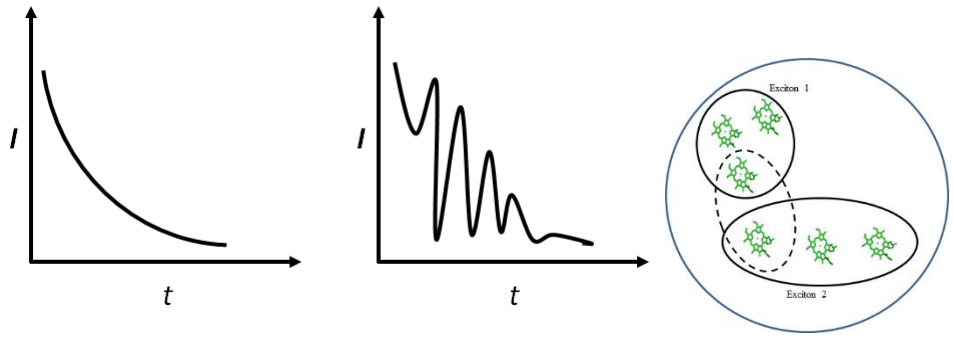

Fig 2:(a); Plot of intensity vs time in the case of incoherent energy transfer (b); Plot of intensity vs time in the case of coherent energy transfer (c); Schematic of what kinds of energy transfer happen inside a single PPC

In fig(b), the oscillations are beats between the excited states of different pigments. The implication is that at any instance of time, excited charge can be spread over spatially separated pigments.

So, how do plants harvest light? Is energy transfer coherent or incoherent? It turns out that plants do both, each kind of energy transfer has its own characteristic limits where it will dominate.

For an incoherent energy transfer, the equilibration of molecule with the environment is on faster timescales than molecule-molecule coupling. This condition constitutes the incoherent limit. The coherent limit is realized when the molecule-molecule coupling is on faster timescales that molecule environment equilibration. In PPCs both of these energy transfers are possible due to the different local environment of each pigment, which decided whether it follows an incoherent or coherent kind of energy transfer. Fig1(c) highlights this point, it shows the possibility of an incoherent energy transfer ("FRET") between two sets of coherently coupled pigments ("Exciton 1" and "Exciton 2") as well as a coherent energy transfer possibility (both represented as the dotted oval).

It should be noted that it is not known whether nature actually relies on coherent energy transfer at all to harvest light. Also, the 2D electronic spectroscopy experiment in which the long-lived coherence was reported involved three femtosecond pulses, two of which were incident on the sample at the same time producing a transient grating of nanometer dimensions, which in turn connected spatially separated molecules, the third pulse probes the molecules on the grating. This by no means is similar to the natural biological environment.

Humanity's effort to make artificial light harvests can be pictorially depicted as follows

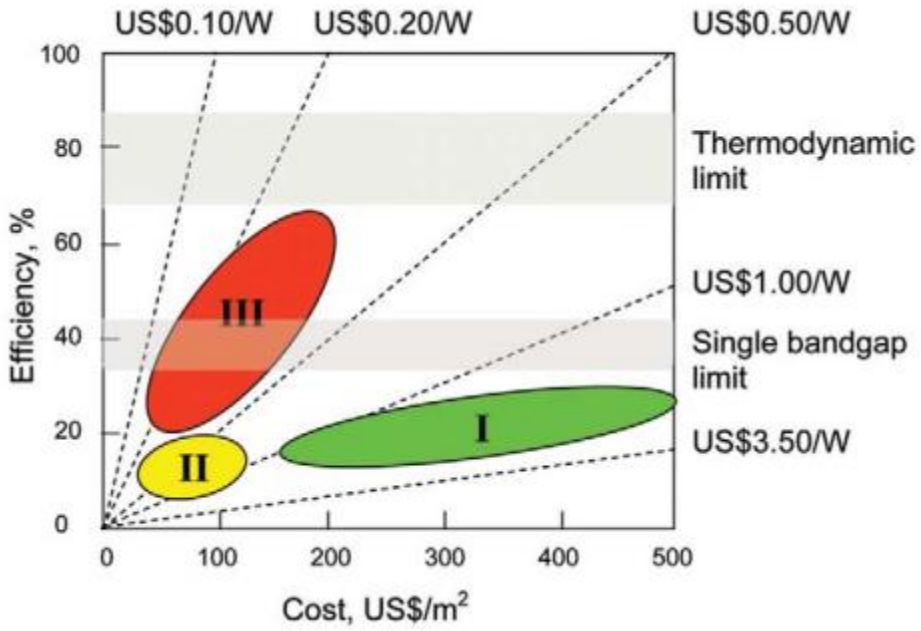

Figure 3; Efficiency vs cost for photovoltaics

Ref. Materialstoday 10,11,42-50 (2007)

I, II and III in Fig3 stand for first, second and third generation respectively. The single bandgap limit is also known as the Shockley-Queisser limit. The silicon solar cell was the most popular, its efficiency is under the Shockley-Queisser limit as well.

The silicon solar cell consisted of two materials, n-doped silicon and p-doped silicon. Doping of semiconductors means adding an impurity to the material, it changes the bandgap as well as the predominant charge carrier. Effective doping can be accomplished with concentrations of one dopant in a few millions of un-doped atoms/molecules. In the case of n-typed silicon, the dopant is an element with one more electron than silicon, e.g. phosphorous. It follows that for p-type silicon, the dopant is an element with one less electron than silicon, e.g. boron. The charge carriers in n-type and p-type silicon are electrons and holes respectively.

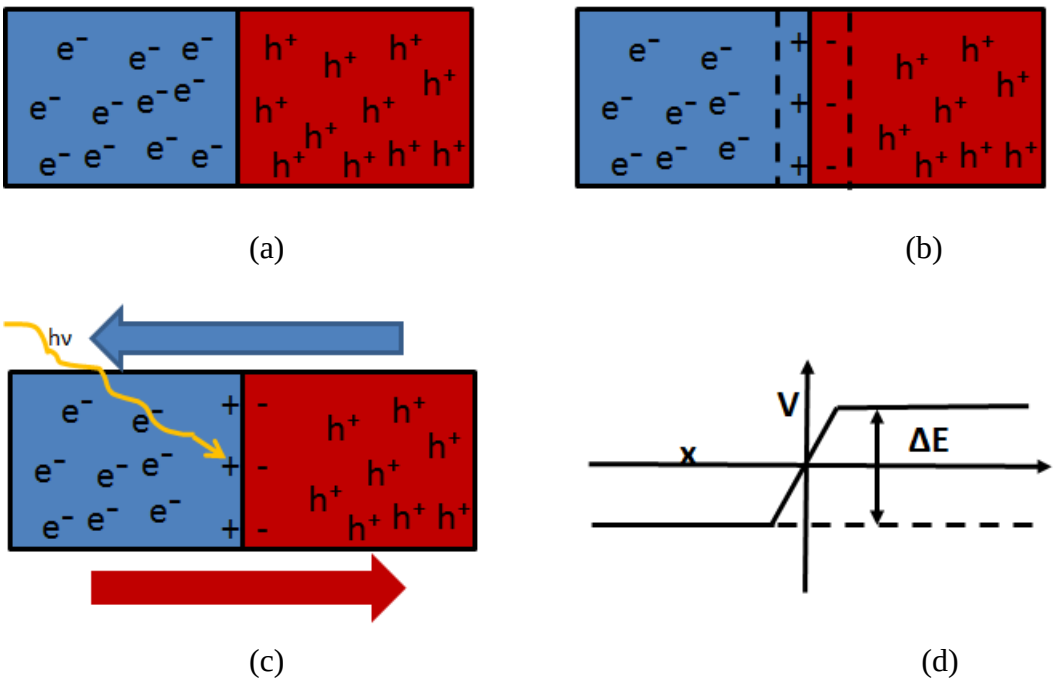

Figure 4: (a); the setup of a silicon solar cell, blue and red represent n-type and p-type silicon. (b); the cell with the depletion region (c); the motion of charge carriers with sunlight (d); the potential vs direction (one dimension) corresponding to the silicon solar cell, where ΔE is the bandgap of silicon

When the n-type and p-type silicon are brought together, the holes in the p-type are free to move to the n-type where they form electron-hole pairs (excitons) and vice-versa. This results in a net negative charge in the p-type and a net positive charge in the n-type, this collective charge layer is known as the depletion region. The depletion region corresponds to a change in potential, indicative of an electric field. Under sunlight, the recombined electrons and holes split and travel in the field created by the depletion region; this results in the holes going back to the p-type and electrons going to the n-type. The charge carries can be extracted at their respective ends and can recombine to do useful work.

There is a limit on the efficiency of silicon solar cells, the Shockley-Quiesser limit theoretically predicts that the maximum efficiency attainable by a silicon solar cell is ~32% [5]. In the paper, Shockley and Quiesser present an idealized case, where the temperature of the cell is 0K and radiation from the sun is received isotopically. Then they extend the description to a more realistic example, where the temperature of the cell is ~300K (close to room temperature) and radiation from the sun is not received isotopically. The assumptions made by them were as follows:

- The input light is from the sun, no focusing optics
- Absorption of the solar cell follows a step function; all photons with energy greater than the bandgap are absorbed
- The only loss to energy is through radiative electron hole recombination

Shockley and Quiesser estimated the rate of radiative recombination through the principle of detailed balance [4]. They considered a region around the silicon solar cell, which was in equilibrium with the cell, this allowed them to equate the black body radiation of the cell to the radiative recombination. In the paper, they first considered an ideal case in which the cell received energy from the sun isotopically and had a temperature of 0K. They then extended the ideal case to the more realistic case in which the radiation received from the sun is anisotropic and the temperature of the cell is ~300K (roughly room temperature). Expressing the equations of the more realistic case in terms of the ideal case, they arrived at the rate of radiative recombination, which turned out to be proportional to the number of charge carriers (both electrons and holes).

Efficiencies of solar cells broke the Shockley-Quiesser limit with the implementation of sensitized solar cells. In sensitized solar cells, a species is excited by light, this species gives its excitation to another species. In the silicon solar cell, silicon had to create the electrons and holes and carry them to their respective terminal. In a sensitized solar cell, one species creates the electron and hole and the other is responsible for the migration to yield useable work [5].

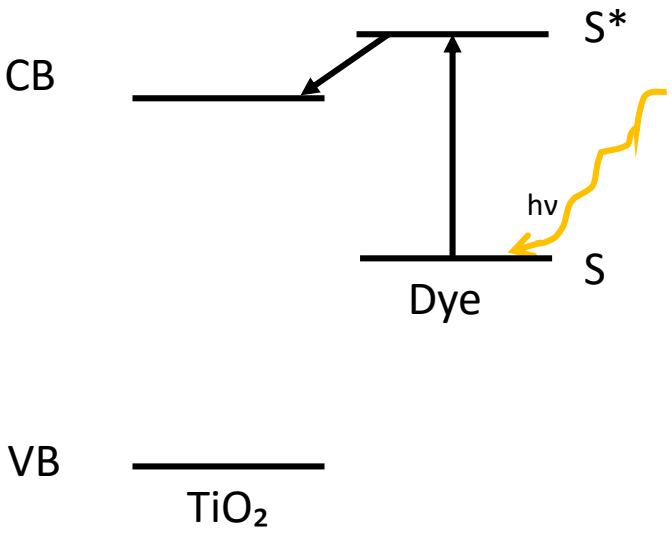

Figure 5: The energy level diagram of a DSSC

In dye sensitized solar cells, the Shockley-Queisser limit is overcome due to different chemicals doing the jobs of charge creation and charge migration. Efficiencies of greater than 10% have been reported for dye-sensitized solar cells.

Chapter 2: Excitons and quantum dots

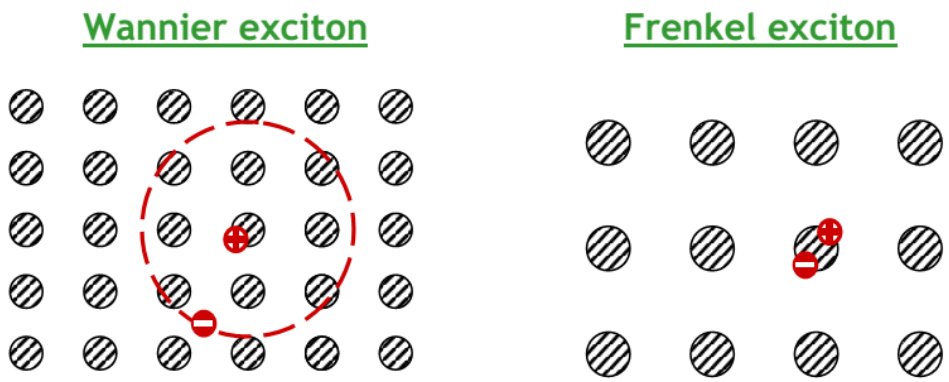

Figure 6: Two kinds of excitons

Ref..http://material-sciences.blogspot.in/2015/05/mengenal-ksiton.html

We have already talked about molecular excitons, a more formal definition is as follows; excitons are quasiparticles which consist of an electron and hole pair. Depending on the length of the exciton (Bohr's excitonic radius), it falls into the two broad categories; Wannier or Frenkel. The length of an exciton depends on the dielectric constant of the material. Wannier excitons correspond to media which have a high dielectric constant, the exciton lengths are around 100Å, with energies of 0.1eV, e.g. liquid xenon. Frenkel excitons are seen in media which have a small dielectric constant, the exciton lengths are around 10Å, with roughly 1eV binding between electrons and holes, e.g. fullerenes.

Quantum dots are semiconductor nanocrystals, comprising of hundreds to thousands of molecules, usually of elements of groups II-VI, III-V, IV-VI e.g. cadmium selenide; CdSe. They are confined in three dimensions, hence they are thought of as a zero dimensional object, a dot [7]. This confinement makes them like a practical particle in a box; which implies that changing the size of a quantum dot, changes the energy level spacing. Once a quantum dot is excited, the excitation is delocalized over all the hundreds to many thousands of molecules; its Bohr's excitonic radius is greater than its size. Quantum dots have been used in many fields, from bio-sensing application to studying charge transfer. They have been known to show both donor and acceptor behavior, quantum dot-quantum dot FRET has been shown as well [8]. Understanding the exciton dynamics within quantum

dots would give us information about excited state dynamics as well as potential solar cell application [9].

Procedure for synthesis of CdSe quantum dots as per [10]:

1. 5ml of octadecene, 30mg of Selenium powder and 0.4ml of Tri-octly phosphine were added to a round bottom flask. They were heated while purging in a nitrogen atmosphere until the solution became colourless, it was left at room temperature.

2. 0.6ml of oleic acid, 10ml of octadecane and 13mg of Cadmium oxide (CdO) were added to another round bottom flask.

3. The flask containing the Cadmium precursor was heated. When the temperature reached 225°C, 1ml of the Selenium stock solution was added, starting the reaction.

4. The solution was filtered at regular intervals.

Procedure for purification of CdSe quantum dots as per [11]:

1. Dilute to 10ml with methanol, centrifuge for 10mins at 5000rpm.
2. The colourless solution was discarded, the remaining solution was diluted to 10ml with toluene and centrifuged for 10mins at 5000rpm.
3. Steps 1 and 2 constitute a single wash, three more washes were done.

The UV-Vis and fluorescence spectra obtained for three CdSe quantum dots are as follows, for 2mm path length cuvette:

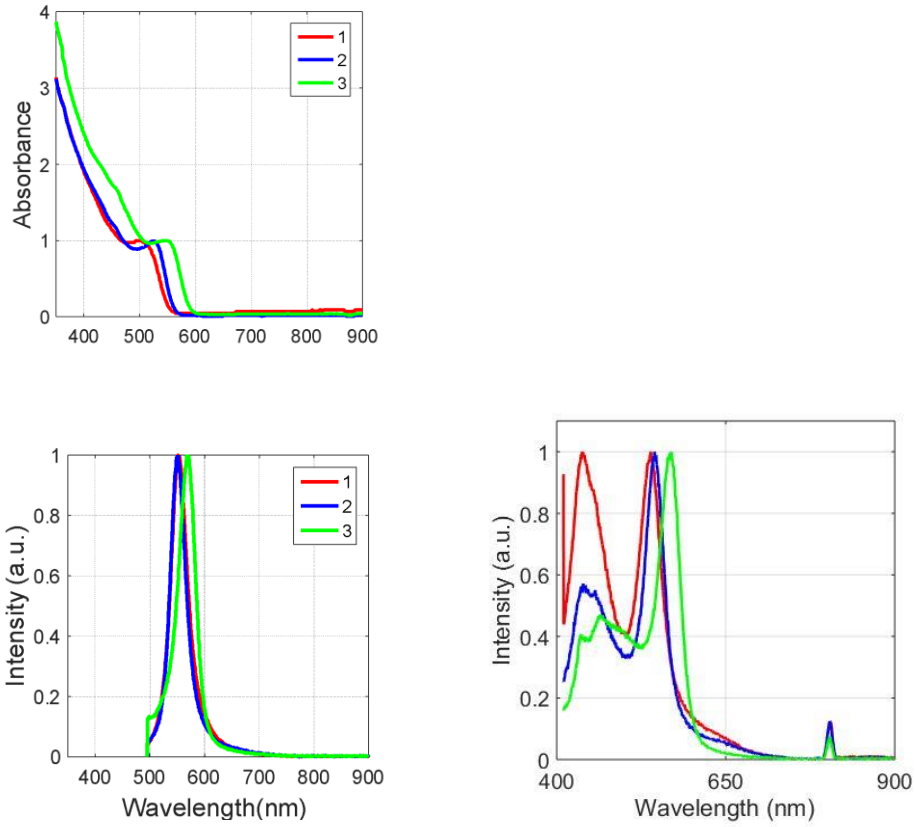

Figure 7: (a) UV-Vis (above) and fluorescence emission spectra (at 485nm excitation) of the three quantum dots (b) Fluorescence emission spectrum at 400nm excitation of the same quantum dots

SNo.	λ_{ex}	λ_{eo}	λ_{e2}
1	499	552	539
2	526	552	545
3	548	570	570

Table1: UV-Vis and fluorescence maxima

Studies on the excited state lifetimes (exciton lifetimes) were carried out using time correlated single photon counting (TCSPC).

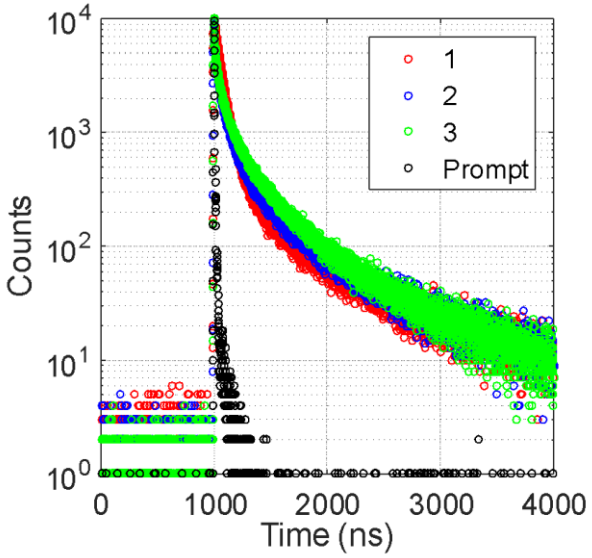

Figure8: TCSPC plots of the sample samples

$\alpha_1 e^{t/\tau_1} + \alpha_2 e^{t/\tau_2} + \alpha_3 e^{t/\tau_3} + \alpha_4 e^{t/\tau_4}$									
α_1	α_2	α_3	α_4	τ_1	τ_2	τ_3	τ_4	$<\tau>$	χ^2
0.39	0.05	0.02	0.54	2.50	11.56	41.07	3.85	4.38	1.031
0.28	0.09	0.02	0.61	2.50	8.78	38.15	0.25	2.44	1.069
0.2	0.1	0.02	0.68	1.89	8.39	31.94	0.19	2.10	1.182

Table2: TCSPC fitting data for the three samples

From X.Peng's paper [12];

$$CdSe\ Diamter\ (in\ nm) = (1.6122 \times 10^{-9})\lambda^4 - (2.6575 \times 10^{-6})\lambda^2 + (1.6242 \times 10^{-9})\lambda^3 - (0.4277)\lambda + (41.57)$$

where λ is the wavelength of the characteristic visible peak in nm. This formula gives us the diameters of 2.34nm, 2.64nm and 3.00nm for samples number 1, 2 and 3 respectively. As per table2, the larger the size of the quantum dot, the less the excited state lifetime, which is the expected trend.

Furthermore, another formula gives us the molar absorption co-efficient (ε):

$$\varepsilon = 5857D^{2.65}$$

This gives us the following molar absorption co-efficient(s) for samples 1,2 and 3; 55453,90187 and 108277.

Using these quantum dots, we also tried to obtain the size distribution through fluorescence spectroscopy. This was done by taking a particular sample and collecting the fluorescence excitation spectrum at different emission wavelengths.

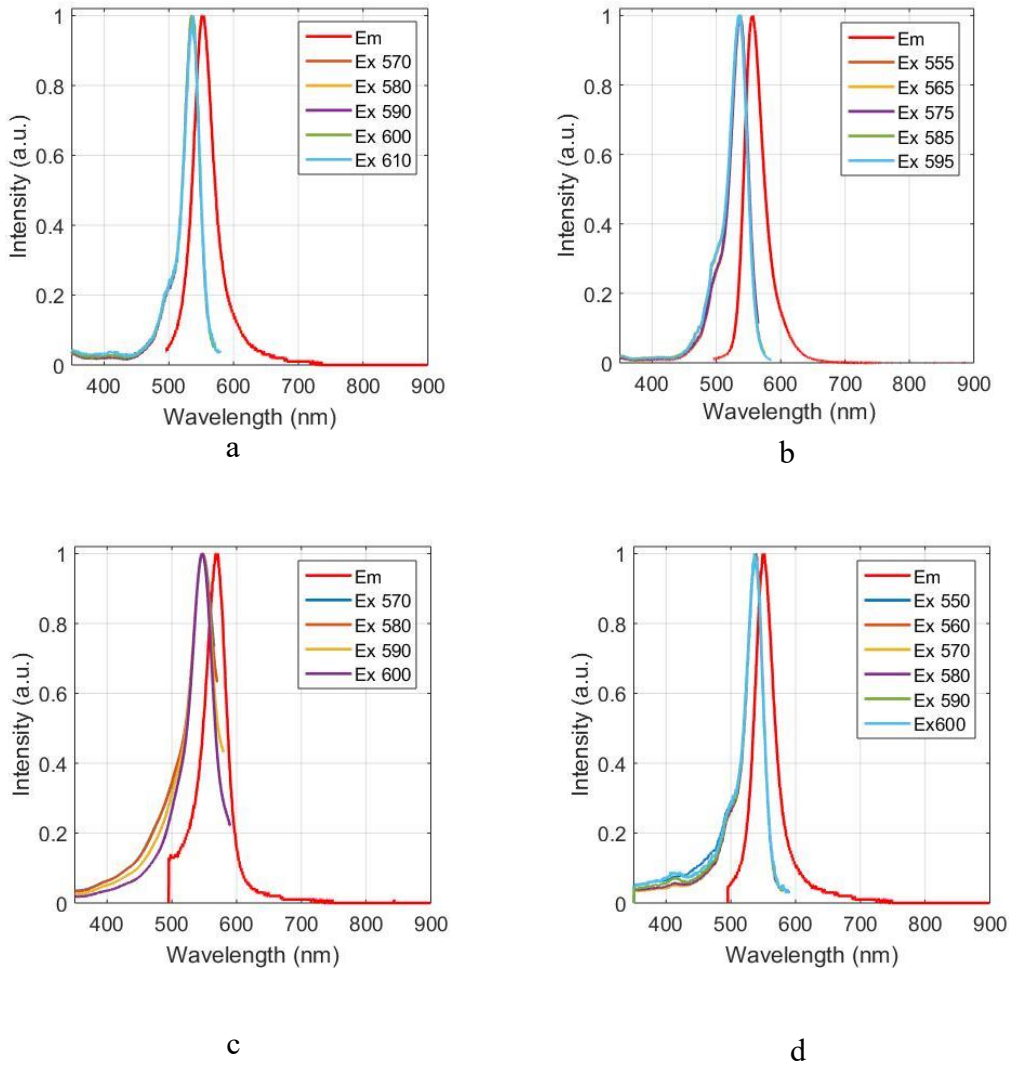

Figure 9: a; Sample 5 b; Mix; 0.3ml of sample 5, 0.3ml of sample 3 and 0.3ml of sample 4 c; Sample 3 d; Sample 4

No pattern in the position of excitation spectra maxima were seen in all these cases. This implies that either the methodology of resolving the distribution was incorrect, or some kind of interaction is taking place between differently distributed particles.

Chapter 3: Pump-probe spectroscopy

The processes that can be observed are only as good as the time resolution of the probe. If the molecular motion of interest happens faster than the time duration of the light being used to observe it, we would not be able to capture the motion itself, similar to taking a photograph with longer shutter time than the actual event. Energy and charge transfer processes, that result in the migration of charge, subsequently producing current, happen on fast timescales. Hence, in order to probe such processes, short pulses need to be used [13].

Electronic spectroscopy provides us with information about the nature of molecular electronic states, thereby shedding light on electronic structure and dynamics upon excitation by light in UV-Vis range. This is experimentally achieved through the use of an excitation source and a detector. A quantity known as transmittance (T) is defined; the ratio of the intensity of light after passing through the sample and the intensity of light before passing through the sample. The output of such an experiment is a plot between the absorbance A ($\log_{10}\frac{1}{T}$) and wavelength (λ) of light used. Such experiments are commonly used in the estimation of concentrations of chromophores (parts of the molecules which absorb in the UV-Vis region), as per Beer-Lambert's law, with ppm (parts per million) resolution. Note; UV-Vis studies electronic absorption, which happens on timescales of $10^{-15} - 10^{-18}$s, the duration of the excitation source is by no means comparable to the process it provides information about. Electronic transitions can be described through excitation from an incident photon, quantized particles of light whose frequency matches the energy difference between the levels involved; this is the frequency domain picture.

Alternatively, transitions can be envisioned in the time domain, this description entails treating the incident light as a wave comprising of a temporally oscillating amplitude and a temporal phase. As this wave hits the sample, its oscillating electric amplitude induces a preferential charge distribution in the sample, inducing a polarization. In a similar way, the induced polarization can be expressed as a wave; with amplitude and phase. The resultant electric field passing through the sample is now, the vector addition of the induced polarization and incident wave. In the case of low intensity incident light, the induced polarization is predominantly proportional to the first power of the incident field (linear) and is in the opposite direction to the incident electric field, due to the conservation of linear momentum; this is known as a phase-matching condition. This is the description of linear

absorption in the time domain. It should be added that once a transition is induced, the excited state has a finite lifetime after which, it falls back to the ground state [14].

Pump-probe spectroscopy is a technique that gives us information about events that happen on femtosecond timescales. It makes use of two femtosecond pulses, the pump and the probe. The probe is delayed with regard to the pump, the delay can be adjusted from 0.3fs-3ns. Two pulses are used to ensure a clear understanding of the initial state, the pump serves to initialize and the probe probes the dynamics of that state.

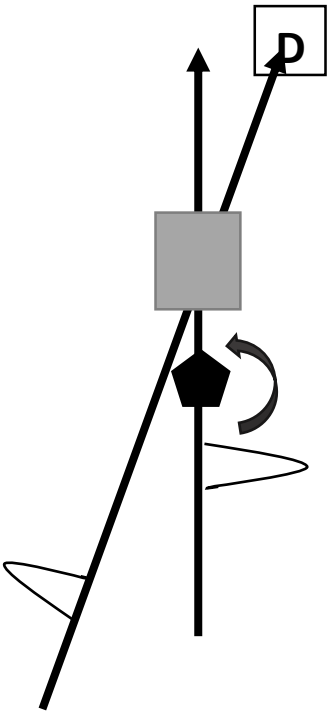

Figure 10: Schematic of a pump-probe setup, the black pentagon denotes a chopper

The output spectrum of a pump-probe experiment is a plot between ΔA, λpu and time (time delay between pump and probe). ΔA gives us information about what sort of absorption/emission is seen. $\Delta A = A_{pump,on} - A_{pump,off}$ Consider the following three level system.

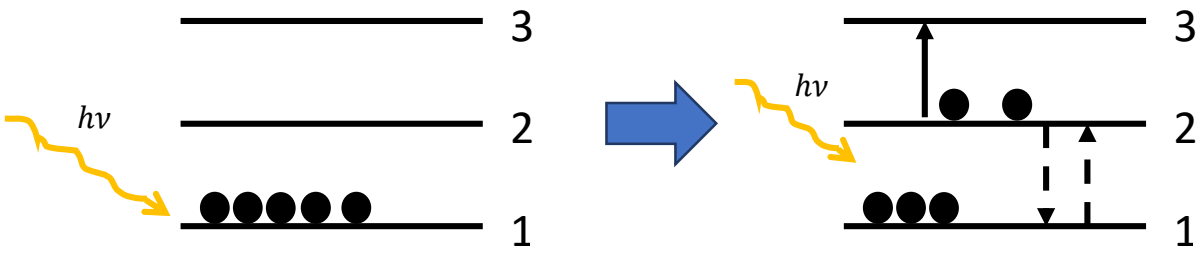

Figure 11: Pump-probe of a three level system

In this particular example, energy levels are equally spaced, the pump and probe are on resonance (ν) with the energy level spacing; $\nu = \nu_{12} = \nu_{23}$. Also, in this particular example all the population is in the ground state. Initially, the pump, excites electrons from 1 to 2. Then the interacts with this new system (in which two electrons are in 2 and three electrons are in 1). The probe can do any of three things; stimulate emission from 2 to 1, re-excite 1 to 2 (known as a ground state bleach) and excited 2 to 3 (excited state absorption). In the case where the probe is blocked, the pump can only cause a 1 to 2 excitation.

For the case of ground state bleach, less population would be available for absorption then initially, so the pump would be absorbed less, hence, $\Delta A_{gsb}<0$.

Similarly, for a stimulated emission, the transmitted light would be more than the incident light, which means that the absorption would be less, hence, $\Delta A_{se}<0$.

The case is different for an excited state absorption, here it is a new absorption and excited state absorptions are greater than ground to excited state absorptions as the magnitude of transition dipoles scale with excited states [15], hence, $\Delta A_{esa}>0$.

In order to find a rough time zero; the time at which both the pump and probe overlap at the same time, a laser dye was used, IR-140.

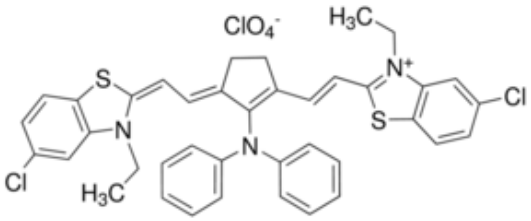

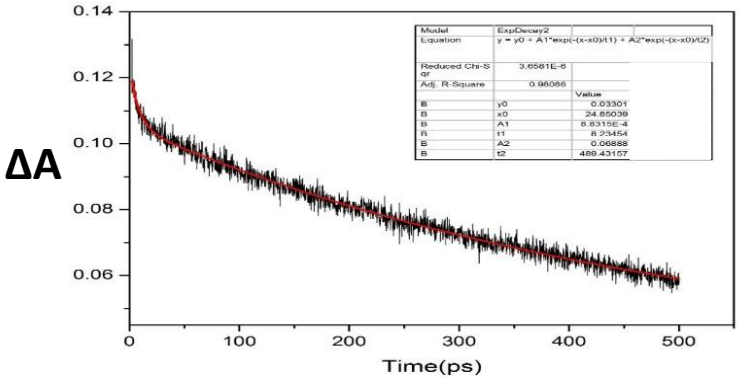

Figure 12: Plot between ΔA and time at 800nm, for an 800-800 pump-probe of IR140

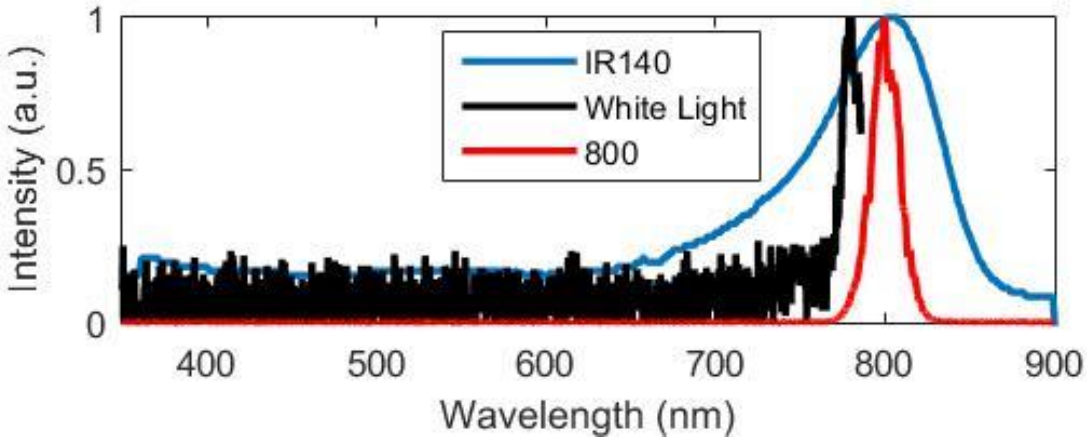

Figure 13: Spectrum of white light, IR140 (absorption) and 800nm

In figure 13, the positive ΔA implies an excited state absorption, this decay can be fitted with a bi-exponential to account for vibrational relaxation and a solvation like process.

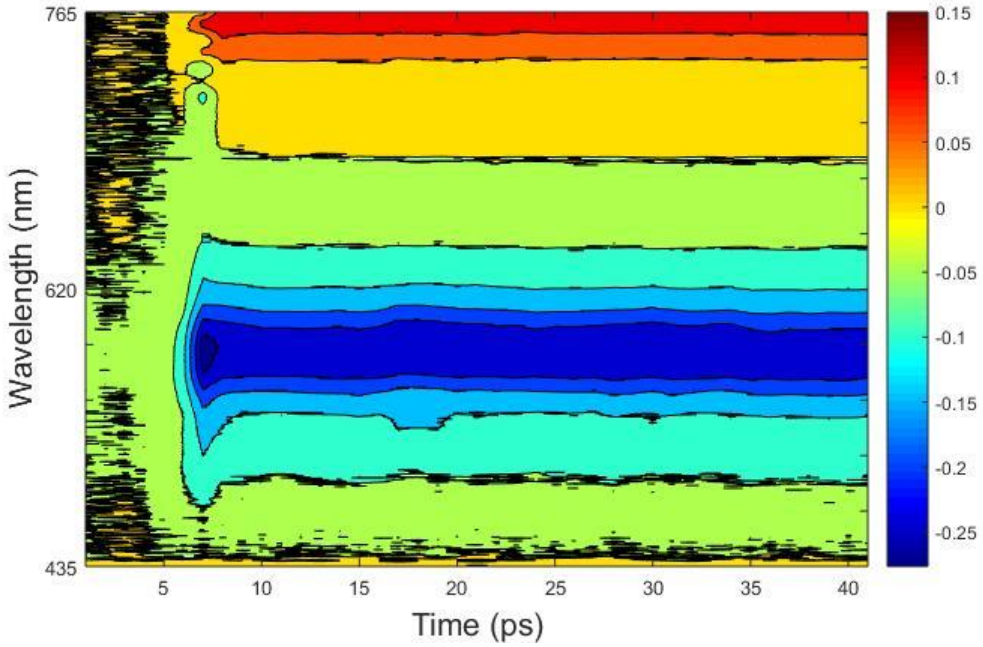

Figure 14: 400-white light, pump-probe spectra of IR140

A concentrated sample of IR140 was used, as absorbance at 400nm was required. This was done to give us a better handle on where time zero was.

Chapter 4: Results and conclusions

The 400-white light pump-probe was used to probe these three quantum dot samples. The three quantum dots showed different absorbance values at 400nm.

	Abs	0.159			Abs	0.41			Abs	0.513
	Abs	0.159			Abs	0.41			Abs	0.513
1	Abs	0.159		2	Abs	0.41		3	Abs	0.513
	Abs	0.159			Abs	0.41			Abs	0.513
	Abs	0.159			Abs	0.41			Abs	0.512
Avg	Abs	0.159		Avg	Abs	0.41		Avg	Abs	0.513
SD	Abs	0		SD	Abs	0		SD	Abs	0

Table 3: Photometry data (from UV-Vis) of the three quantum dots taken at 400nm

The pump-probe data was scanned at different times for each sample. The time intervals which were used were:

1. 0-1ps at 1fs steps
2. -1-10ps at 10fs steps
3. -10-100ps at 100fs steps
4. -100-1000ps at 1000fs steps

The screenshots of these plots and respective corresponding $\Delta\, OD$ v/s time at signal maximum for all time delays (1-4) were as follows:

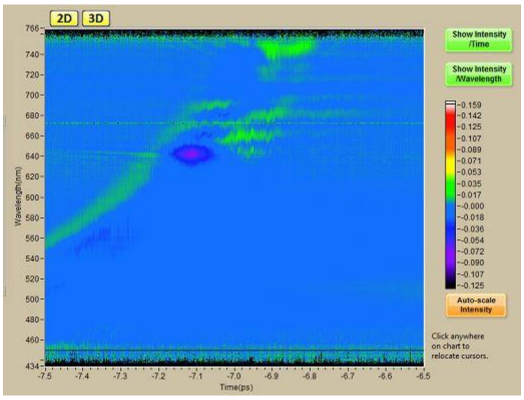

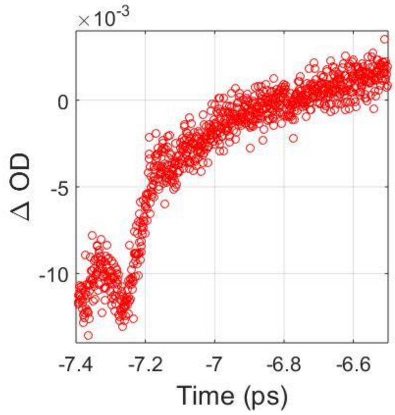

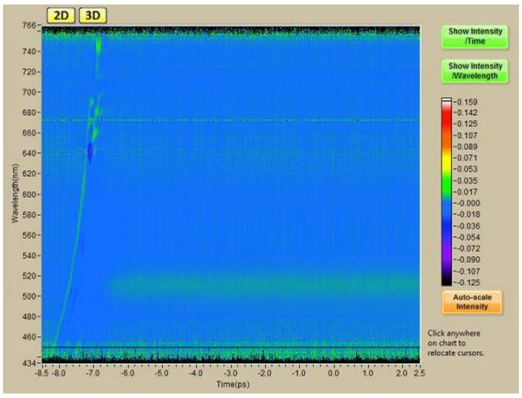

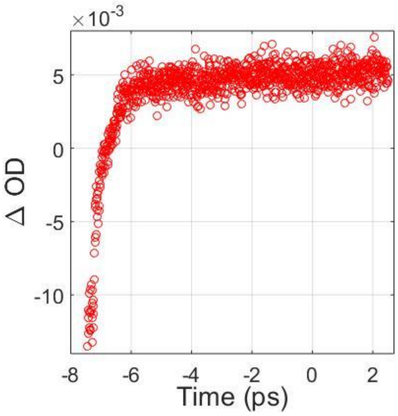

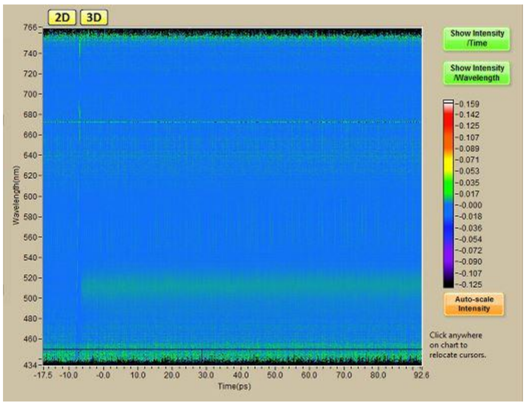

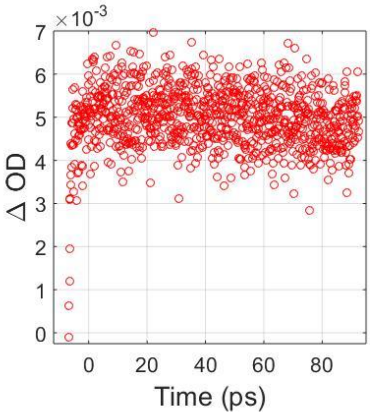

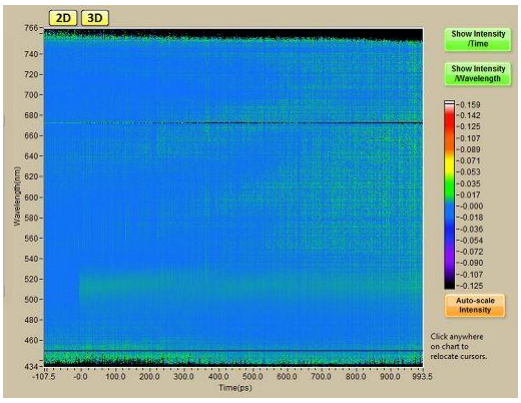

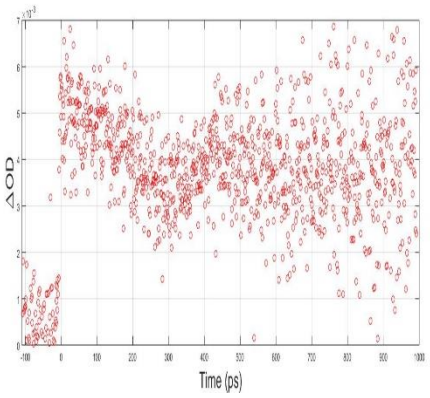

Figure 15: 400-white light sample 1 at different times and corresponding $\Delta\, OD$ v/s time at 510nm.

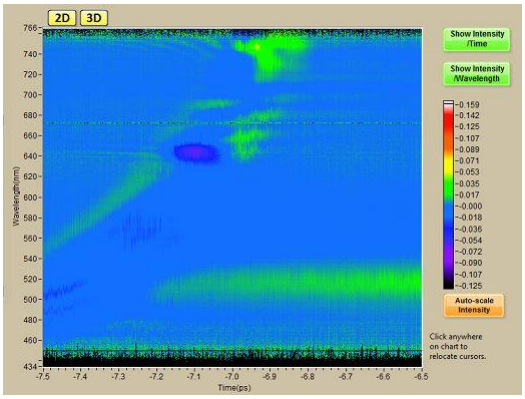

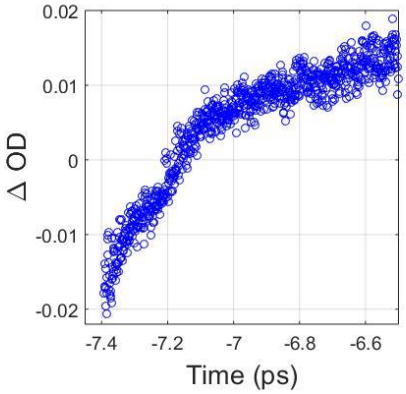

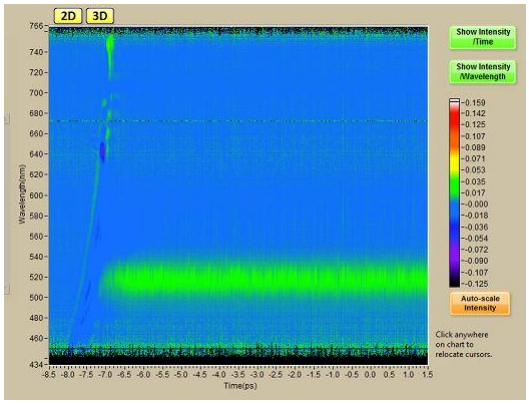

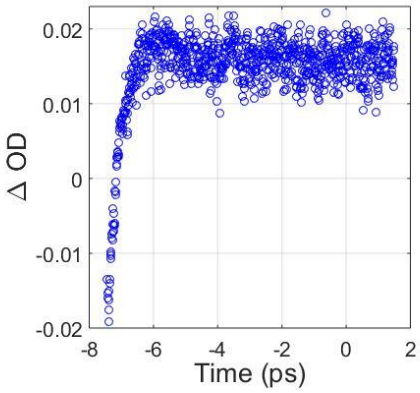

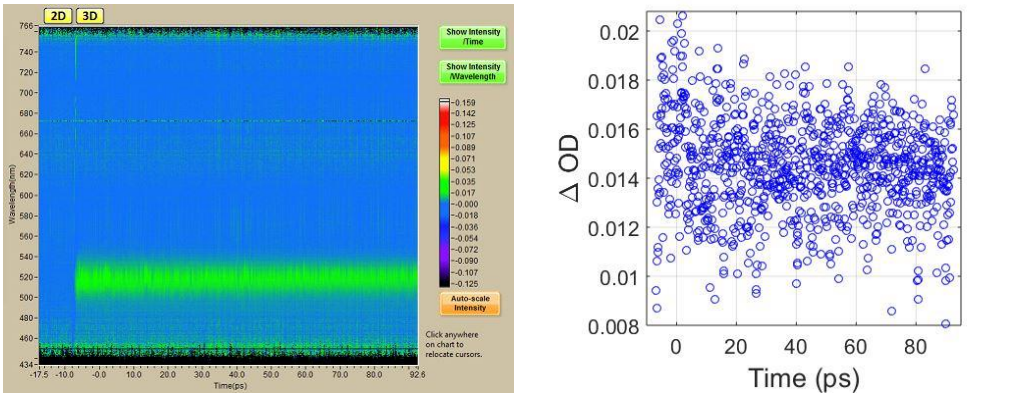

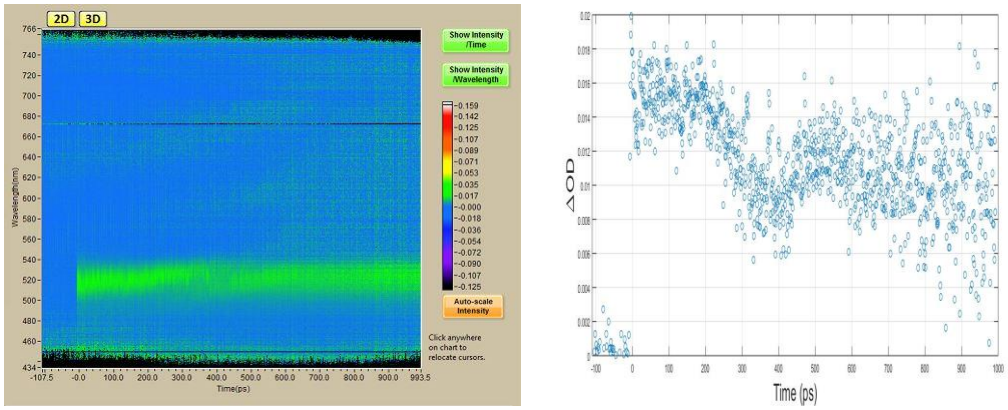

Figure 16:400-white light Pump-probe of Sample 2 at different times and corresponding $\Delta\, OD$ v/s time at 520nm.

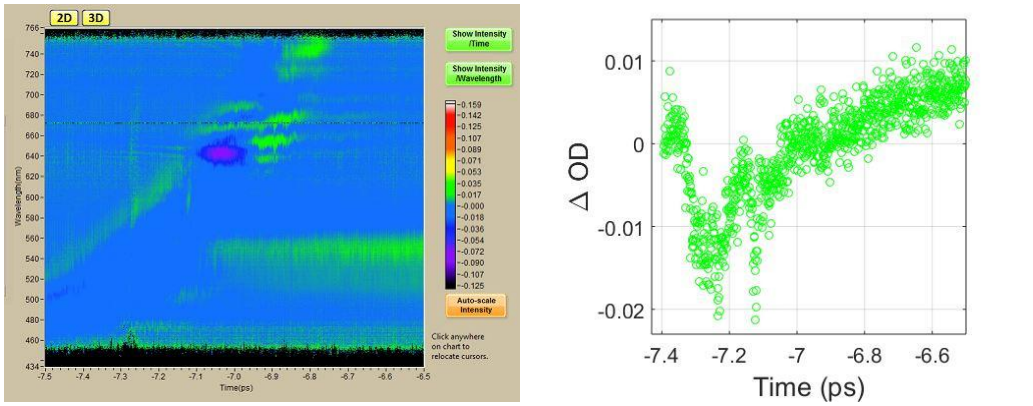

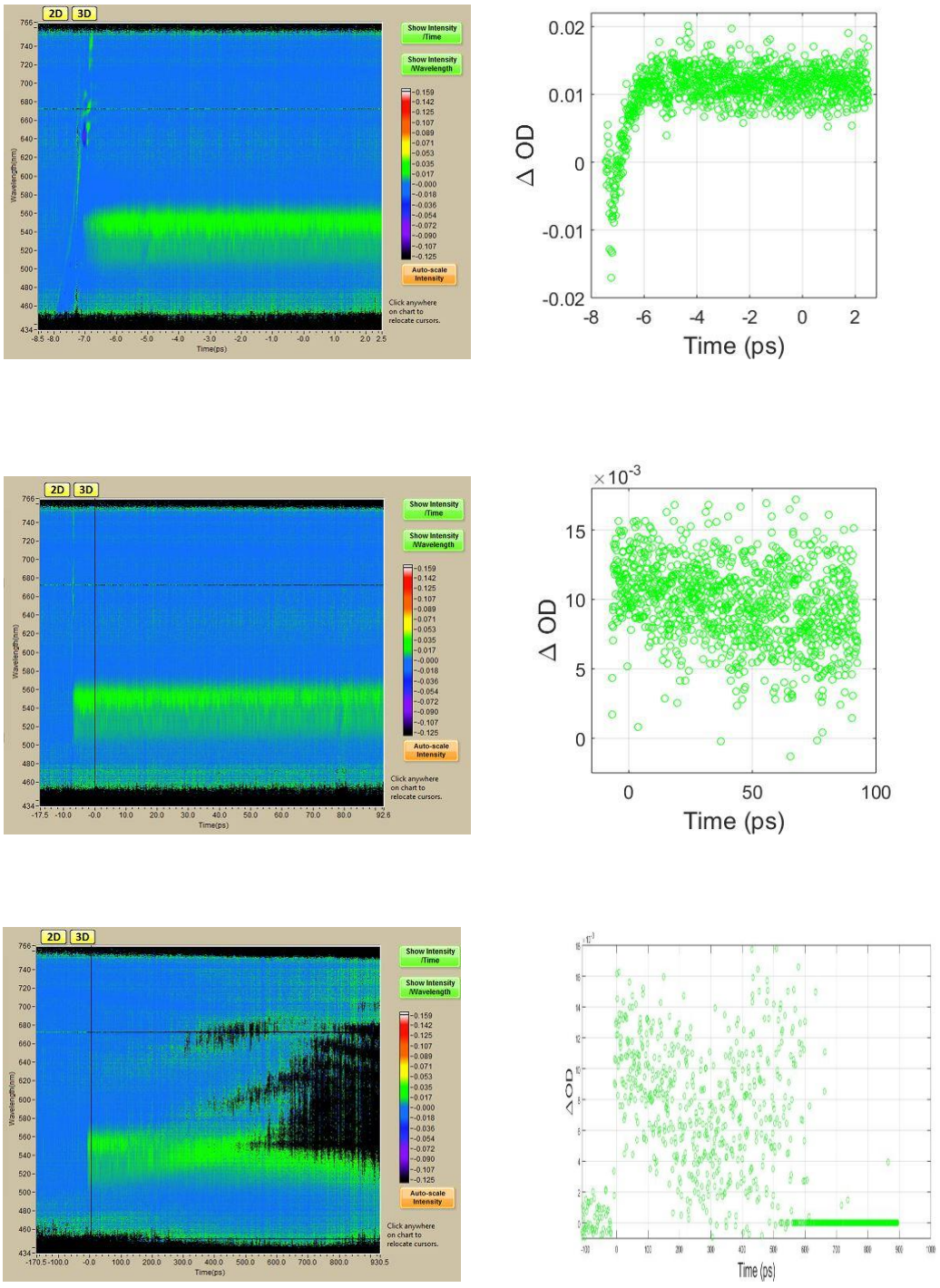

Figure 17: 400-white light Pump-probe of Sample 3 at different times and corresponding $\Delta\, OD$ v/s time at 560nm

Conclusions and future prospects:

From the above data it is apparent that there are exciton dynamics in very fast timescales; of the order of a few femtoseconds. These dynamics manifest themselves differently in the three samples; in the first and third samples signatures similar to ground state bleach/stimulated emission whereas the second sample shows dynamics of the like of excited state absorption. Also, in the case of the first and third samples, there are two characteristic dynamical processes corresponding to different spectral humps.

The further directions for this project point towards obtaining better temporal resolution of the processes; this can be achieved through the use of a spectrally short pump as well as a spectrally short probe (which probes the region of interest).

To understand the nature of the size distribution among the quantum dot samples, a two pulse photon echo could be used as there is a clean separation between the kinds of broadening which we would like to resolve.

Bibliography:

(1) Mirkovic, T.; Ostroumov, E. E.; Anna, J. M.; van Grondelle, R.; Govindjee; Scholes, G. D. *Chem. Rev.* **2016**, acs.chemrev.6b00002.

(2) Förster, T. *Ann. Phys.* **1948**, *437*, 55–75.

(3) Engel, G.; Calhoun, T.; Read, E.; Ahn, T. *Nature* **2007**, *446* (7137), 782–786.

(4) Fassioli, F.; Dinshaw, R.; Arpin, P. C.; Scholes, G. D. *J. R. Soc. Interface* **2014**, *11* (92), 20130901.

(5) Shockley, W.; Queisser, H. J. *J. Appl. Phys.* **1961**, *32* (3), 510–519.

(6) Grätzel, M. *J. Photochem. Photobiol. C Photochem. Rev.* **2003**, *4* (2), 145–153.

(7) Alivisatos, A. P. *Science (80-.).* **1996**, *271* (5251), 933–937.

(8) Kagan, C. R.; Murray, C. B.; Nirmal, M.; Bawendi, M. G. *Phys. Rev. Lett.* **1996**, *76*, 1517–1520.

(9) Kamat, P. V. *J. Phys. Chem. Lett.*, **2013**, *4* (6), 908–918

(10) Nordell, K. J.; Boatman, E. M.; Lisensky, G. C. *J. Chem. Educ.* **2005**, *82* (11), 1697.

(11) Shakeri, B.; Meulenberg, R. W. *Langmuir* **2015**, *31* (49), 13433–13440.

(12) Yu, W. W.; Qu, L.; Guo, W.; Peng, X. *Chem. Mater.* **2003**, *15* (14), 2854–2860.

(13) Baskin, J. S.; Zewail, A. H. *J. Chem. Educ.* **2001**, *78* (6), 737.

(14) De, A. K. *J. Postdr. Res.* **2014**, *2* (7), 23–28.

(15) Bott, R. *Hamm and Zanni*; 2014.